Published in final edited form as:

J Pharm Sci. 2017 February ; 106(2): 639–644. doi:10.1016/j.xphs.2016.09.030.

Label-Free Measurements of Tenofovir Diffusion Coefficients in a Microbicide Gel using Raman Spectroscopy

Oranat Chuchuen[1], **Jason R. Maher**[1], **Morgan G. Simons**[1], **Jennifer J. Peters**[1], **Adam P. Wax**[1], and **David F. Katz**[1,2,*]

[1]Department of Biomedical Engineering, Duke University, Durham, North Carolina, United States of America

[2]Department of Obstetrics and Gynecology, Duke University, Durham, North Carolina, United States of America

Abstract

Confocal Raman spectroscopy was implemented in a new label-free technique to quantify molecular diffusion coefficients within gels. A leading anti-HIV drug, tenofovir, was analyzed in a clinical microbicide gel. The gel was tested undiluted, and in 10 – 50%w/w dilutions with vaginal fluid simulant to capture the range of conditions likely occurring *in vivo*. The concentration distributions of tenofovir in gel over time and space were measured and input to a mathematical diffusion model to deduce diffusion coefficients. These were $3.16 \pm 0.11 \times 10^{-6}$ cm^2/s in undiluted gel, and increased by 11 – 46% depending upon the extent of dilution. Results were interpreted with respect to traditional release rate measurements in devices such as Franz cells. This comparison highlighted an advantage of our assay in that it characterizes the diffusive barrier within the gel material itself; in contrast, release rate in the traditional assay is affected by external conditions, such as drug partitioning at the gel/liquid sink interface. This new assay is relevant to diffusion in polymeric hydrogels over pharmacologically relevant length scales, e.g. those characteristic of topical drug delivery. Resulting transport parameters are salient measures of drug delivery potential, and serve as inputs to computational models of drug delivery performance.

Graphical abstract

*Corresponding author.

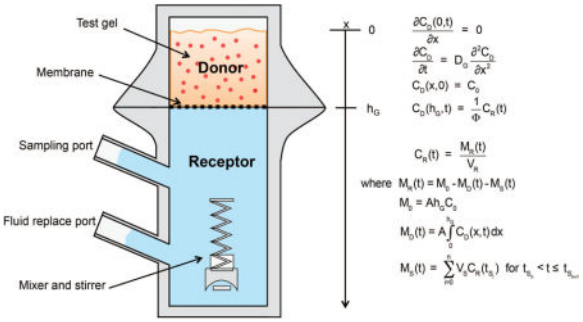

Keywords

Drug transport; Raman spectroscopy; Diffusion; Hydrogels; HIV/AIDS; Microbicides; Pharmacokinetics

Introduction

Microbicides can provide an alternative (to vaccines) and important modality for prevention of sexually transmitted HIV and possibly other pathogens.[1] They occupy a unique space in the HIV prevention network, and are among a small number of prevention methods that could be used independently or in conjunction with other forms of prophylactics. When applied vaginally, they are under primary control of a female user, who would not have to rely upon her sexual partner to provide HIV protection. Multiple drugs and delivery vehicles are being evaluated for potential microbicide products. The most advanced are a tenofovir gel and a dapivirine ring, both of which have demonstrated efficacy in at least one trial.[2,3] Both drugs act within the vaginal, and potentially rectal, mucosa by inhibiting reverse transcriptase production by virions in early stages of their interaction with infectable host cells. Results from gel trials have been mixed, in part because of limitations of user adherence.[4] Still, the familiarity of vaginal gels to women and their current use for multiple gynecological purposes motivate continued evaluation of them as a modality for delivery of microbicides.

Initial analysis of the drug delivery capability of prototype products typically includes measuring the release rate of drug from its vehicle.[5–7] This is often performed in a vertical diffusion cell (e.g., a Franz cell) which exposes an upper gel layer to a lower stirred fluid sink compartment, and measures the accumulating drug concentration in the sink vs. time. For standardized testing in which the gel layer thickness and the drug permeability of the supporting membrane in the Franz cell are invariant, this release rate can be used meaningfully to compare prototype products for a given drug. However, the release rate parameter cannot be used to predict drug delivery by a gel into target tissues, only to contrast its potential with that of other gels. Accurate prediction is central to rational product design, and benefits substantially from a deterministic, analytic approach to the drug delivery process. This includes not just release from the vehicle but drug transport into and through target tissue. Computational modeling can help achieve this. The modeling requires input parameters including fundamental transport properties, such as drug diffusion and partition coefficients, in all compartments of the problem.[8–10] While modeling predictions can

provide comprehensive understanding of how product properties govern drug delivery, the drug diffusion coefficient in a gel per se can be a more robust alternative to the traditional release rate parameter in characterizing drug delivery potential.

In pharmacological processes, drugs may migrate through gels that are not just their vehicles but are also target matrices, e.g. the vitreous of the eye or the cervical mucus.[11] Transport often occurs over length scales on the order of a few hundred microns. Drug diffusion in gels is sensitive to the length scale over which it is evaluated.[12] However, there has been relatively little work on measuring diffusion over the intermediate length scale relevant to the microbicide delivery problem. Such knowledge is vital to understanding microbicide gel functionality and to development and evaluation of candidate products. The present study was designed to address this shortcoming. Using a custom designed chamber and optical system, we applied confocal Raman spectroscopy to measure the spatiotemporal history of tenofovir transport within a clinical gel.

Raman spectroscopy (RS) has been shown to be of practical value for concentration profiling in polymeric matrices.[13,14] This technique detects the frequency change of photons that undergo Raman scattering, a form of inelastic scattering that results from changes in the vibrations of chemical bonds.[15,16] The intensity of Raman scattering is proportional to the concentration of the detected molecule or chemical bond in solution.[17] RS has begun to emerge as a useful tool to obtain molecular concentration profiles in biomedical systems including fluids, gels, and tissues. For example, Kwak and Lafleur used RS to study the diffusion of polyethylene glycol (PEG) of different molecular weights through Ca-alginate gels.[13] Recently, our group applied high-resolution confocal RS (CRS) to measure concentrations of microbicide drugs in liquids and their concentration distributions in porcine tissues, using a Transwell configuration.[18,19] Here, we constructed a custom horizontal diffusion cell enabling measurements of spatiotemporal concentration distributions of the microbicide drug tenofovir in its clinical vaginal gel.[2,20,21] These data were fit with a time-dependent diffusion model to obtain diffusion coefficients. The gels were tested undiluted, and at 10%w/w (1:9 VFS:gel) to 50%w/w (1:1 VFS:gel) dilutions with vaginal fluid simulant (VFS).[22] These dilutions simulated the range of conditions experienced by the gel within the vaginal canal *in vivo*.[23] Gel dilution and possible gel swelling associated with dilution could alter drug diffusion coefficients and, therefore, transport of drug within and out from the gels.

Materials and Methods

Materials and diffusion chamber

Tenofovir gel and a drug free placebo gel of the same composition were kindly provided by Professor Lisa C. Rohan (University of Pittsburgh School of Pharmacy). The tenofovir gel was developed by the CONRAD Program (Arlington, VA) for use in clinical studies.[2,20,21] The gel (pH 4.4) was formulated with 1%w/w tenofovir (MW 287), 20%w/w glycerol, hydroxyethylcellulose, edetate disodium, citric acid, methylparaben, propylparaben, and purified water. Both tenofovir and placebo gels were diluted with vaginal fluid simulant (pH 4.2)[22] to investigate the effect of dilution on gel transport properties. Dilution samples were prepared to contain 10%, 20%, 30%, or 50% by weight of VFS and 90%, 80%, 70%, or 50%

by weight of gel, respectively. These dilutions simulated the range of physiological dilutions expected *in vivo*.[22–24] Each sample was thoroughly mixed by vortexing. A gel diffusion chamber was constructed specifically for use in these experiments (Figure 1). It consisted of two custom-manufactured quartz rectangular capillary cells (Starna Cells, Atascadero, CA) that were placed in an aluminum mounting. Each cell had an internal rectangular channel running through the center of the cell with dimensions of 0.3 mm × 8 mm × 20.1 mm. One cell acted as the donor compartment while the other was the receptor compartment. The contact surface between the two cells served as the interface across which drug diffused from the donor compartment into the receptor compartment.

Diffusion experiments

Gel was loaded into each diffusion cell with a syringe and silicone tubing. The donor cell was loaded with the tenofovir gel while the receptor compartment was loaded with the placebo gel. Care was taken during gel loading to avoid the formation of bubbles in the medium, which could affect the molecular diffusion of the target drug. The non-interface ends of the cells were securely sealed with a waterproof tape to prevent gel dehydration. The diffusion chamber was placed on a temperature-controlled motorized stage to maintain the gel at physiological temperature, 37.0 ± 0.5°C, throughout each experiment. A custom built CRS-OCT (confocal Raman spectroscopy and optical coherence tomography) instrument integrated with a white-light camera was used to acquire data in this study.[19] The axial and lateral resolutions of the CRS subsystem are 19 and 3 μm, respectively. The OCT subsystem has an axial resolution of 8 μm and a lateral resolution of 40 μm, and the white-light camera offers a lateral resolution of 2 μm. Prior to CRS measurements, the OCT subsystem was used to visualize the diffusion chambers to verify proper alignment of their central channels. The white-light camera was used to locate and establish the interface of the two diffusion cells at the onset of each experiment. The motorized translation stage was controlled with custom software written in LabView (National Instruments, Austin, TX). This enabled data collection from precise locations within the donor and receptor cells over a period of up to 24 hours.

Timing of each experiment began at the onset of donor-receptor cell contact. Measurements were acquired at 150 μm below the surfaces of both the donor and receptor cells as functions of time and distance from the interface between the cells. At each location, the total exposure time was 0.75–3 minutes; the exposure time was increased for higher dilutions to achieve an adequate signal-to-noise ratio.

In order to deduce absolute concentrations of tenofovir, calibration curves were constructed with homogeneous solutions of tenofovir in gel. Separate calibration curves were created for each studied dilution by diluting, with slow mixing, the VFS-diluted gels with a VFS-diluted placebo gel. Calibration measurements were performed at the beginning of each experiment using the same data acquisition conditions as those used for the test gel dilution.

Raman spectral analysis

Spectral analysis was implemented using Matlab (MathWorks, Natick, MA). A custom Matlab script was used to process raw spectral data, as outlined previously.[19] The

contributions of tenofovir to each Raman spectrum were established by ordinary least squares fitting. A representative fit with the Raman spectral contributions of Tenofovir, gel, and vaginal fluid simulant is displayed in Figure 2. Calibration curves (e.g., Figure 3) related the spectral contribution of tenofovir to a known concentration in the measurement volume. Using these calibration curves, concentration profiles of tenofovir in the diffusion cell were extracted from the spectral data.

Computation of diffusion coefficients

The measured drug concentrations over time and space in the donor (C_D) and receptor compartments (C_R) were fit with a drug diffusion model containing the two contiguous compartments (Figure 4). Inputs to the model were: the initial drug concentration in the donor compartment (C_0) and the receptor compartment (zero) as well as the lengths of the diffusion cells (h_D and h_R). A built-in partial differential equation (PDE) solver in Matlab, “pdepe”, was utilized to numerically solve the PDEs. Nonlinear data fitting was performed using a Matlab built-in function, “lsqnonlin”. The diffusion coefficient was determined via nonlinear optimization using a trust-region-reflective algorithm, which minimizes the sum of squared residuals between the measured concentration values and those predicted based on the model.

Results

Raman spectra of tenofovir distributions suggested that tenofovir concentrations were changing along the length of the diffusion cells. A set of representative Raman spectra acquired in real-time during a typical experiment is displayed in Figure 5. For each measurement cycle, the peak intensities of tenofovir at 725 cm^{-1} [18,19] decreased from the donor towards the receptor compartments, while other peaks of gel remained unchanged.

A representative spatiotemporal distribution of tenofovir concentration in gels is displayed in Figure 6. As expected, the concentrations of tenofovir were dependent upon the distance from the donor/receptor interface. Over time, the donor concentrations decreased while the receptor concentrations increased towards the interfacial concentrations, which were approximately 50% of the initial concentrations. The concentrations of tenofovir at the interface remained relatively unchanged throughout the experiments.

The full spatiotemporal data set suggests that the transport of tenofovir in the clinical gel exhibited diffusion-like behavior. Across all experiments, measured concentration values fit reasonably well with the diffusion model (e.g., Figure 6), with coefficients of determination (R^2) ranging from 0.95 to 0.99. The precision (using the coefficient of variation) of the determined diffusion coefficients ranged from 3 to 5%. Dilution with vaginal fluid simulant increased diffusion coefficients by 11 – 46% (Table 1 and Figure 7), depending upon the extent of dilution. As expected, dilution caused gel swelling and a subsequent increase in the transport rate.

Discussion

We have introduced a new method for measuring drug diffusion coefficients in gels over length scales (on the order of a few hundred microns) relevant to topical drug delivery to mucosal and other surfaces. Specifically, diffusion coefficients were determined here for a clinical vaginal gel containing the microbicide drug tenofovir. Following *in vivo* insertion, microbicide gels are diluted by intravaginal fluids.[23,24] Dilution changes gel properties, including rheological properties (that govern flow over the surfaces)[9,10,23] and molecular diffusion coefficients within the gels (as measured in this study). The assay here is precise enough to characterize the increase in the tenofovir diffusion coefficient due to physiologically relevant dilution with a simulant for those vaginal fluids. The changing behavior of the diffusion coefficient with respect to extent of dilution is likely to be pharmacologically relevant because it governs the rate of mass transport of the drug out of the gel. As seen in Table 1 and Figure 7, there was a trend: as the gel became more diluted with vaginal fluid simulant, the drug diffusion coefficient increased. A simple estimate of consequent diffusion kinetics can be made using the familiar mean free path formula for self-diffusion, $\mathrm{x}=\sqrt{2\mathrm{Dt}}$ where x is the root mean square distance diffused, D is the diffusion coefficient and t is time.[25] Thus, for example, an increase of 46% in the diffusion coefficient (viz. due to 50% dilution) would result in a 21% greater distance traveled by drug through the gel during a given time interval.

The increase in the diffusion coefficient suggests that dilution with vaginal fluid simulant caused gel swelling, resulting in less resistance to diffusion (random walk) by individual tenofovir molecules within the gel. Interestingly, while lower amounts of dilution (<20%) produced a linear change in the diffusion coefficient vs. dilution, additional dilution resulted in a slower change. This suggests that the polymer network structure of the gel was undergoing greater changes vs. dilution at lower dilutions, and that the change in molecular configuration began to stabilize at higher dilutions.

The new assay presented here is an extension and expansion of the familiar use of Franz cells to measure drug release from test vehicles. In that traditional method, a layer of the vehicle of interest (the donor compartment) is held in place on a membrane within the Franz cell, and drug concentration is measured vs. time in a stirred liquid sink compartment below (the receptor). Results are often plotted vs. the square root of time, in accord with the solution for the drug release problem given in the Higuchi equation.[26,27] The slope of a linear fit to such data is interpreted as the “release rate” with units of drug mass / [cross sectional area • (time)$^{0.5}$]. Mechanistically, this is an approximation for short times (viz. $\mathrm{t} \ll \frac{\mathrm{L}^2}{36\mathrm{D}}$ where L is the gel thickness).[25] In the problem here, this short time scale ranges from less than 2 minutes (for thin gel layers ~ 1 mm) to ~2 hours (for thick layers ~ 1 cm). Such times are much shorter than those typically used in Franz cell based assays. Thus, the accuracy of the Higuchi equation-based release rate can be compromised in those assays.

A number of factors govern the drug release rate parameter obtained using a Franz cell. For a gel these include: gel layer thickness (proportional to loaded gel volume); sink (receptor) compartment depth; type and amount of the sink fluid; cross sectional areas of the gel and

liquid sink; volume and frequency of liquid sampling; drug diffusion coefficient in the gel; partitioning effects of the membrane that supports the gel layer; and effects of any gel swelling or shrinkage that could occur due to differences in osmolality between the gel and sink liquid. These latter effects include time-dependent changes in gel layer thickness and the drug diffusion coefficient within the gel (as demonstrated in data from the study here). Thus, the drug release rate is a lumped parameter that embodies a complex physicochemical process. In contrast, the diffusion coefficient derived from the RS-based assay in this paper is a fundamental transport property independent of those factors.

We can illustrate the limitations of traditional methods that employ a Franz-like diffusion cell to study drug release from a gel formulation using a mathematical model of drug diffusion (see Appendix, Figure S1). Traditional release data can be fit with this model to deduce a diffusion coefficient within the gel. Figure 8 demonstrates the effect of drug partitioning at the membrane on the computed diffusion coefficient within the gel in the Franz cell. This partition coefficient represents a combined effect of the membrane resistance and the differential drug solubility between the gel and liquid sink compartments that could be affected by progressive gel swelling (or shrinkage), as well as other factors such as the amount of air bubbles at the membrane. Thus, this partition coefficient is time-dependent and can vary for each experiment depending upon the type of membrane and the sink fluid used. At lower values of the partition coefficient, the Franz cell-determined diffusion coefficient is higher than that determined by RS. As the partition coefficient increases, the Franz cell-determined diffusion coefficient of tenofovir decreases and stabilizes to values about one fourth of the RS-determined ones. Since this partition coefficient cannot be measured precisely, the accuracy of the determination of the diffusion coefficient from the Franz cell data is compromised.

In the RS assay there is no membrane at the donor/receptor interface, and both compartments contain the same type of gel. Thus, there is no drug partitioning at the interface, and the RS-determined diffusion coefficient is independent of the partition coefficient. The only two inputs to the diffusion model (Figure 4) are the initial drug concentration (C_0) and the lengths of the diffusion cells (h_D and h_R); these parameters are constant and time-invariant. It is straightforward to model the RS assay and to deduce the diffusion coefficient (the only unknown parameter) from the RS data, which contain a few hundred data points per experiment (vs. 8 – 12 points for a typical Franz cell experiment).[5–7]

Notably, a gel with a higher Franz cell-based release rate may not necessarily have a higher drug diffusion coefficient; thus, it might not be more effective in delivering drug to tissue *in vivo* – the higher release rate could be due to higher drug partitioning between that gel and sink fluid. This result is a caveat to sole reliance upon Franz cell data when inferring drug release from gels into other media or tissues.

If drug partitioning at the membrane is comparable across gels, and if drug partitioning and the diffusion coefficient in gel do not change over time with gel swelling, then Franz cell results do provide an objective means of comparing potential for release performance for a drug across multiple gels. However, the drug release rate lumped parameter cannot be used to objectively predict drug delivery to tissue quantitatively. For example, it cannot be

translated into decisions in the gel design process related to pharmacokinetic performance per se or effects of applied gel volume.[9] Such decisions require more fundamental information about drug mobility within the gels, in conditions that simulate those *in vivo*. This is where use of the new assay presented here fits. In particular, characterization of the diffusion coefficient (a fundamental mass transport property) can be input to deterministic modeling of the overall process of drug mass transport from a gel into a target matrix (e.g mucosal tissue) and thus predict pharmacokinetic performance.[8–10] From a more empirical perspective, comparing diffusion coefficients of a drug across multiple gels provides a more robust characterization of potential for *in vivo* drug release and delivery than comparing values of release rates obtained from Franz cells.

To the best of our knowledge, the tenofovir diffusion coefficient in aqueous solution has not yet been reported in literature. However, one may deduce the diffusion coefficient of tenofovir in water using its solvent accessible surface area (SASA) to compute an effective hydrodynamic size[28,29] and employing the Stokes-Einstein relationship.[25,30] The hydrodynamic radius of tenofovir in water (pH 4.2–4.4) is estimated to be 5.7 A°.[31] Thence, the Stokes-Einstein equation predicts the diffusion coefficient of tenofovir in water at 37°C to be 5.76×10^{-6} cm^2/s. The diffusion coefficient of tenofovir in undiluted gel was thus 0.55 ± 0.02 of that in water. It increased by ~46% to 0.80 ± 0.03 in 1:1 dilution of gel. These ratios were determined previously for the diffusion of fluorescein (322 Da) and 10kD dextran within three different microbicide gel formulations using post photoactivation scanning (PPS).[32] The ratios varied between gels and increased upon dilution. In undiluted gels, they were found to range from 0.54 to 0.68 for fluorescein and from 0.44 to 0.57 for dextran. In 1:1 diluted gels, they increased to 0.70 – 0.81 for fluorescein. Thus, the degree of the gel restrictive effect on particle diffusion and its change upon dilution determined from the present assay appear to be within a physically meaningful range of published data for particle diffusion in microbicide gels.

Other microbicide drugs differ from tenofovir in size and structure, from small molecules (e.g. Dapivirine, MIV 150, IQP-0528) to much larger proteins (e.g. Griffithsin[33]). The assay here offers promise in evaluating gel delivery of those drugs as well, including how it is influenced by *in vivo* dilution (given suitable Raman-friendly optical behavior, of course).

The RS-based diffusion assay proposed in this paper offers promise for measuring transport properties of multiple drugs and other molecules in hydrogels. Unlike many traditional approaches, this method does not involve tagging or altering the drug or the gel material itself. Such processes can alter the mobility of studied particles in gels, and that artifact can compromise the fidelity of the diffusion coefficients deduced.[34] RS offers a noninvasive alternative to identifying and quantifying concentrations of chemical compounds in a matrix without altering them to enable measurement. Results from the RS method can be input to deterministic compartmental models that predict details of product PK.[8–10] In turn, those predictions inform our fundamental understanding of drug delivery and the development of products and selection of their dosage regimens, as part of a rational design process.

Supplementary Material

Refer to Web version on PubMed Central for supplementary material.

Acknowledgments

We are grateful to Professor Lisa C. Rohan and Ms. Lin Wang (University of Pittsburgh School of Pharmacy) for providing us the tenofovir and placebo gels and the CONRAD programs for donations of tenofovir used in this study. We thank Dr. Marinella Sandros in accommodating our use of the Horiba Xplora Confocal Raman Microscope at the Joint School of Nanoscience and Nanoengineering (University of North Carolina, Greensboro and North Carolina A&T State University, Greensboro, NC) to obtain preliminary data in this project. We also acknowledge Mr. Michael Desoto and Dr. Marcus Henderson (Duke University, Department of Biomedical Engineering) for their help and useful insights provided throughout the project. Support was provided by NIH HD072702.

Appendix

A vertical analyte diffusion cell (e.g. a Franz cell) is modeled as consisting of two compartments: donor and receptor (Figure S1). The receptor compartment is continuously stirred, so that analyte concentration within it is spatially homogenous. Consider a gel layer of thickness h_G supported by a membrane in the cell. The receptor (sink) fluid volume is V_R. An unsteady one-dimensional diffusion equation can be employed to describe the time-dependent concentration distribution in the donor compartment (C_D). The time-dependent concentration in the receptor compartment (C_R) is computed by dividing the time-dependent analyte mass in the receptor (M_R) by the volume of the receptor fluid (V_R). M_R is derived from mass balance, subtracting the mass lost during fluid sampling $M_S(t)$ at discrete sampling times (t_s) and the instantaneous mass still in the gel, $M_D(t)$, from the initial mass, M_0. A time-dependent boundary condition with a partition coefficient (Φ) is applied at the interface between the donor and receptor compartments. This partitioning is due to differential drug solubility in the donor vs receptor media and the properties of the supporting membrane.

The partial differential equation and boundary conditions were first rewritten as difference equations, which were then solved by a built-in function, ode15s in Matlab software (MathWorks, Natick, MA). The accumulated, total mass of released drug was computed by summing the mass in the receptor, $M_R(t)$, and the sampled mass, $M_S(t)$. To determine the diffusion coefficient from a traditional drug release assay in this device, release data[7] were fitted with the above model via nonlinear curve fitting, utilizing a Matlab built-in function, lsqcurvefit. That function employs a trust-region-reflective algorithm to minimize the sum of squared residuals between the experimental data and predicted concentration values based on the model. Results and comments are presented in the Discussion section.

References

1. Buckheit RW, Watson KM, Morrow KM, Ham AS. Development of topical microbicides to prevent the sexual transmission of HIV. Antiviral research. 2010; 85(1):142–158. [PubMed: 19874851]
2. Karim QA, Karim SSA, Frohlich JA, Grobler AC, Baxter C, Mansoor LE, Kharsany ABM, Sibeko S, Mlisana KP, Omar Z, Gengiah TN, Maarschalk S, Arulappan N, Mlotshwa M, Morris L, Taylor D, Grp CT. Effectiveness and Safety of Tenofovir Gel, an Antiretroviral Microbicide, for the Prevention of HIV Infection in Women. Science. 2010; 329(5996):1168–1174. [PubMed: 20643915]

3. Baeten JM, Palanee-Phillips T, Brown ER, Schwartz K, Soto-Torres LE, Govender V, Mgodi NM, Matovu Kiweewa F, Nair G, Mhlanga F. Use of a Vaginal Ring Containing Dapivirine for HIV-1 Prevention in Women. New England Journal of Medicine. 2016
4. Dai JY, Hendrix CW, Richardson BA, Kelly C, Marzinke M, Chirenje ZM, Marrazzo JM, Brown ER. Pharmacological measures of adherence and risk of HIV acquisition in the VOICE study. Journal of Infectious Diseases. 2015:jiv333.
5. Rohan LC, Moncla BJ, Kunjara Na Ayudhya RP, Cost M, Huang Y, Gai F, Billitto N, Lynam JD, Pryke K, Graebing P, Hopkins N, Rooney JF, Friend D, Dezzutti CS. In vitro and ex vivo testing of tenofovir shows it is effective as an HIV-1 microbicide. PLoS One. 2010; 5(2):e9310. [PubMed: 20174579]
6. Cost M, Dezzutti CS, Clark MR, Friend DR, Akil A, Rohan LC. Characterization of UC781-tenofovir combination gel products for HIV-1 infection prevention in an ex vivo ectocervical model. Antimicrob Agents Chemother. 2012; 56(6):3058–3066. [PubMed: 22430977]
7. Dezzutti CS, Rohan LC, Wang L, Uranker K, Shetler C, Cost M, Lynam JD, Friend D. Reformulated tenofovir gel for use as a dual compartment microbicide. Journal of Antimicrobial Chemotherapy. 2012; 67(9):2139–2142. [PubMed: 22581908]
8. Gao Y, Katz DF. Multicompartmental pharmacokinetic model of tenofovir delivery by a vaginal gel. PLoS One. 2013; 8(9):e74404. [PubMed: 24040241]
9. Gao Y, Yuan A, Chuchuen O, Ham A, Yang KH, Katz DF. Vaginal deployment and tenofovir delivery by microbicide gels. Drug delivery and translational research. 2015; 5(3):279–294. [PubMed: 25874971]
10. Katz DF, Yuan A, Gao Y. Vaginal drug distribution modeling. Advanced drug delivery reviews. 2015; 92:2–13. [PubMed: 25933938]
11. Dunmire EN, Plenys AM, Katza DF. Spectrophotometric analysis of molecular transport in gels. Journal of Controlled Release. 1999; 57(2):127–140. [PubMed: 9971891]
12. Yuan F, Krol A, Tong S. Available space and extracellular transport of macromolecules: effects of pore size and connectedness. Annals of biomedical engineering. 2001; 29(12):1150–1158. [PubMed: 11853267]
13. Kwak S, Lafleur M. Raman spectroscopy as a tool for measuring mutual-diffusion coefficients in hydrogels. Applied spectroscopy. 2003; 57(7):768–773. [PubMed: 14658654]
14. Bell SE, Dennis AC, Fido LA, Malcolm RK, Sirimuthu NM, Toner CF, Woolfson AD. Characterization of silicone elastomer vaginal rings containing HIV microbicide TMC120 by Raman spectroscopy. J Pharm Pharmacol. 2007; 59(2):203–207. [PubMed: 17270074]
15. Raman CV. A change of wave-length in light scattering. Nature. 1928; 121:619–619.
16. Szymanski, HA. Raman spectroscopy: theory and practice. Springer Science & Business Media; 2012.
17. McCreery RL. Photometric standards for Raman spectroscopy. Handbook of vibrational spectroscopy. 2002
18. Chuchuen O, Henderson MH, Sykes C, Kim MS, Kashuba AD, Katz DF. Quantitative analysis of microbicide concentrations in fluids, gels and tissues using confocal Raman spectroscopy. PLoS One. 2013; 8(12):e85124. [PubMed: 24386455]
19. Maher JR, Chuchuen O, Henderson MH, Kim S, Rinehart MT, Kashuba AD, Wax A, Katz DF. Co-localized confocal Raman spectroscopy and optical coherence tomography (CRS-OCT) for depth-resolved analyte detection in tissue. Biomedical optics express. 2015; 6(6):2022–2035. [PubMed: 26114026]
20. Van Damme L, Corneli A, Ahmed K, Agot K, Lombaard J, Kapiga S, Mookho Malahleha, Fredrick Owino, Rachel Manongi, Jacob Onyango, Lucky Temu, Modie Constance Monedi, Paul Mak'Oketch, Mankalimeng Makanda, Ilse Reblin, Shumani Elsie Makatu, Lisa Saylor, Haddie Kiernan, Stella Kirkendale, Christina Wong, Robert Grant, Angela Kashuba, Kavita Nanda, Justin Mandala, Katrien Fransen, Jennifer Deese, Tania Crucitti, Timothy D Mastro, Douglas Taylor. Preexposure prophylaxis for HIV infection among African women. New England Journal of Medicine. 2012; 367(5):411–422. [PubMed: 22784040]

21. Rees H, Delany-Moretlwe S, Baron D, Lombard C, Gray G, Myer L, Panchia R, Schwartz J, Doncel G. Conference on Retroviruses and Opportunistic Infections (CROI), Seattle, WA. 2015:23–26.
22. Owen DH, Katz DF. A vaginal fluid simulant. Contraception. 1999; 59(2):91–95. [PubMed: 10361623]
23. Lai BE, Xie YQ, Lavine ML, Szeri AJ, Owen DH, Katz DF. Dilution of microbicide gels with vaginal fluid and semen simulants: effect on rheological properties and coating flow. J Pharm Sci. 2008; 97(2):1030–1038. [PubMed: 17724667]
24. Drake TK, Shah T, Peters JJ, Wax A, Katz DF. Measuring dilution of microbicide gels with optical imaging. PLoS One. 2013; 8(12):e82213. [PubMed: 24340006]
25. Truskey, GA., Yuan, F., Katz, DF. Transport phenomena in biological systems. Pearson/Prentice Hall; Upper Saddle River NJ: 2004.
26. Higuchi T. Rate of Release of Medicaments from Ointment Bases Containing Drugs in Suspension. J Pharm Sci. 1961; 50(10):874–&. [PubMed: 13907269]
27. Siepmann J, Peppas NA. Higuchi equation: derivation, applications, use and misuse. International journal of pharmaceutics. 2011; 418(1):6–12. [PubMed: 21458553]
28. Ferrara P, Apostolakis J, Caflisch A. Evaluation of a fast implicit solvent model for molecular dynamics simulations. Proteins: Structure, Function, and Bioinformatics. 2002; 46(1):24–33.
29. Hellweg T, Eimer W, Krahn E, Schneider K, Müller A. Hydrodynamic properties of nitrogenase—the MoFe protein from Azotobacter vinelandii studied by dynamic light scattering and hydrodynamic modelling. Biochimica et Biophysica Acta (BBA)-Protein Structure and Molecular Enzymology. 1997; 1337(2):311–318. [PubMed: 9048909]
30. Mohr CW, Vogt RD, Røyset O, Andersen T, Parekh NA. An in-depth assessment into simultaneous monitoring of dissolved reactive phosphorus (DRP) and low-molecular-weight organic phosphorus (LMWOP) in aquatic environments using diffusive gradients in thin films (DGT). Environmental Science: Processes & Impacts. 2015; 17(4):711–727. [PubMed: 25789463]
31. Marvin16.4.11.0.2016. ed.: ChemAxon (http://www.chemaxon.com).
32. Geonnotti AR, Furlow MJ, Wu T, DeSoto MG, Henderson MH, Kiser PF, Katz DF. Measuring macrodiffusion coefficients in microbicide hydrogels via postphotoactivation scanning. Biomacromolecules. 2008; 9(2):748–751. [PubMed: 18193840]
33. Emau P, Tian B, O'Keefe BR, Mori T, McMahon JB, Palmer KE, Jiang Y, Bekele G, Tsai CC. Griffithsin, a potent HIV entry inhibitor, is an excellent candidate for anti-HIV microbicide. Journal of medical primatology. 2007; 36(4–5):244–253. [PubMed: 17669213]
34. Gajraj A, Ofoli RY. Effect of extrinsic fluorescent labels on diffusion and adsorption kinetics of proteins at the liquid-liquid interface. Langmuir. 2000; 16(21):8085–8094.

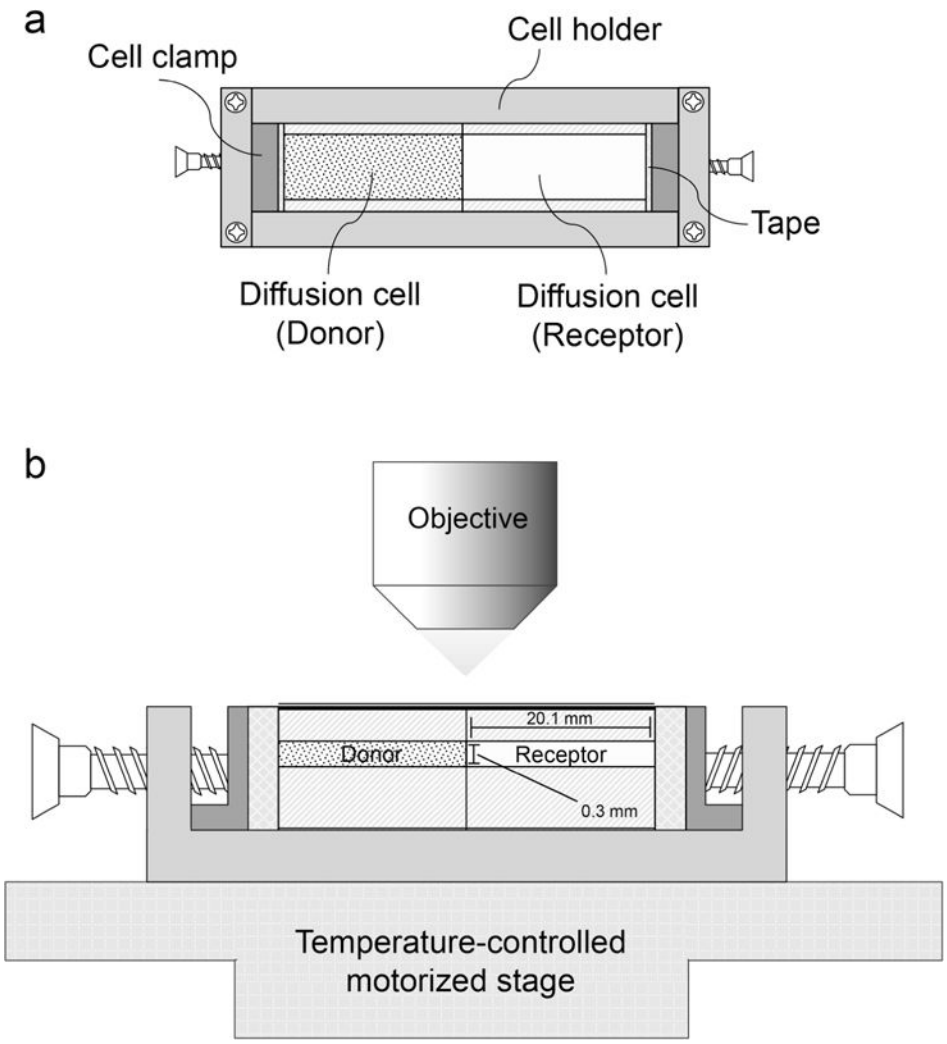

Figure 1.

Custom-built diffusion chamber used to perform the gel diffusion experiments.

(A) Schematic of the diffusion cell for measuring drug transport and the diffusion coefficients in gels. The donor compartment is loaded with tenofovir gel, and the receptor is filled with a placebo gel of the same composition, minus the drug. (B) Side view of the diffusion cell that is set up on a temperature-controlled motorized stage.

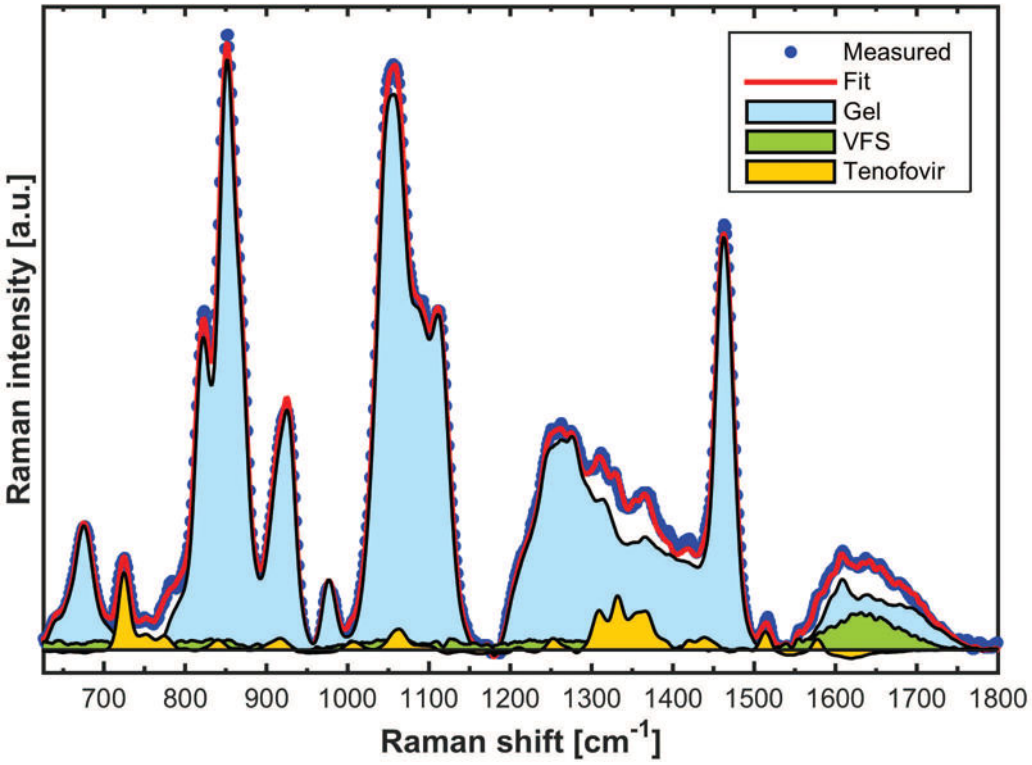

Figure 2.

A representative Raman spectrum acquired during a typical experiment, fitted with pure spectral components of tenofovir, placebo gel, and vaginal fluid simulant (VFS). Ordinary least squares fitting yielded Raman spectral contributions of each of the spectral components. Spectra were cropped for clarity of presentation.

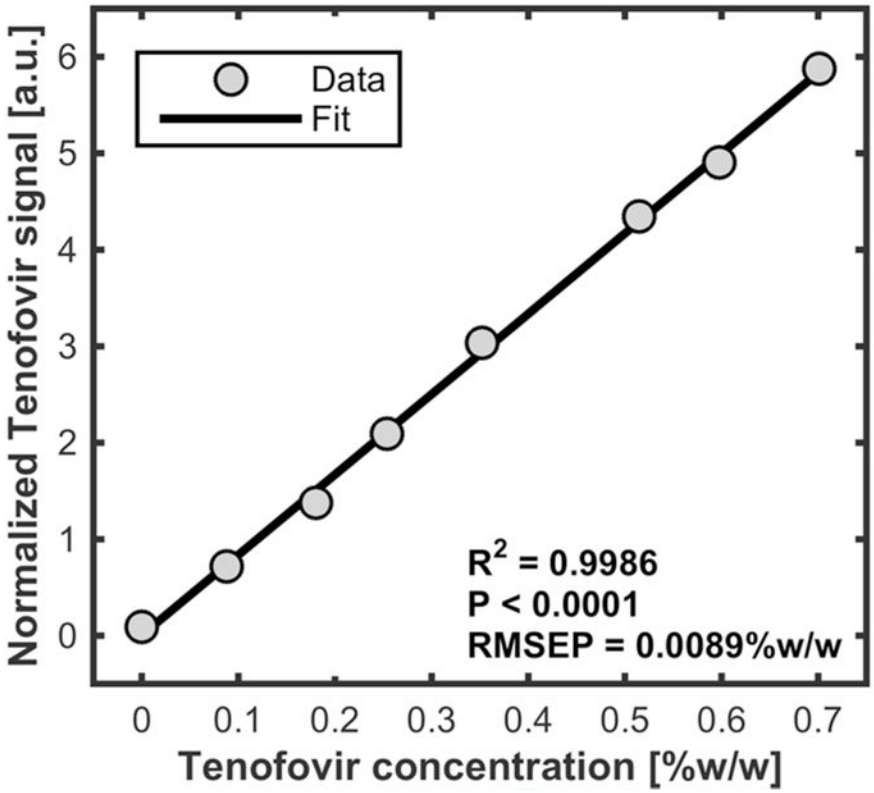

Figure 3.

A representative calibration curve of tenofovir in (30% diluted) gel for performing quantitative analysis of tenofovir concentration distributions in gel. Calibration measurements were acquired at the beginning of each experiment. Each data point represents mean of 5–6 acquisition frames. A strong linear dilution response ($R^2 > 0.99$, $P < 0.0001$) for concentrations of tenofovir in the gel was observed. The root mean squared error of prediction (RMSEP) represents the prediction accuracy of tenofovir concentration in gel. Calibration curves were obtained for each studied dilution.

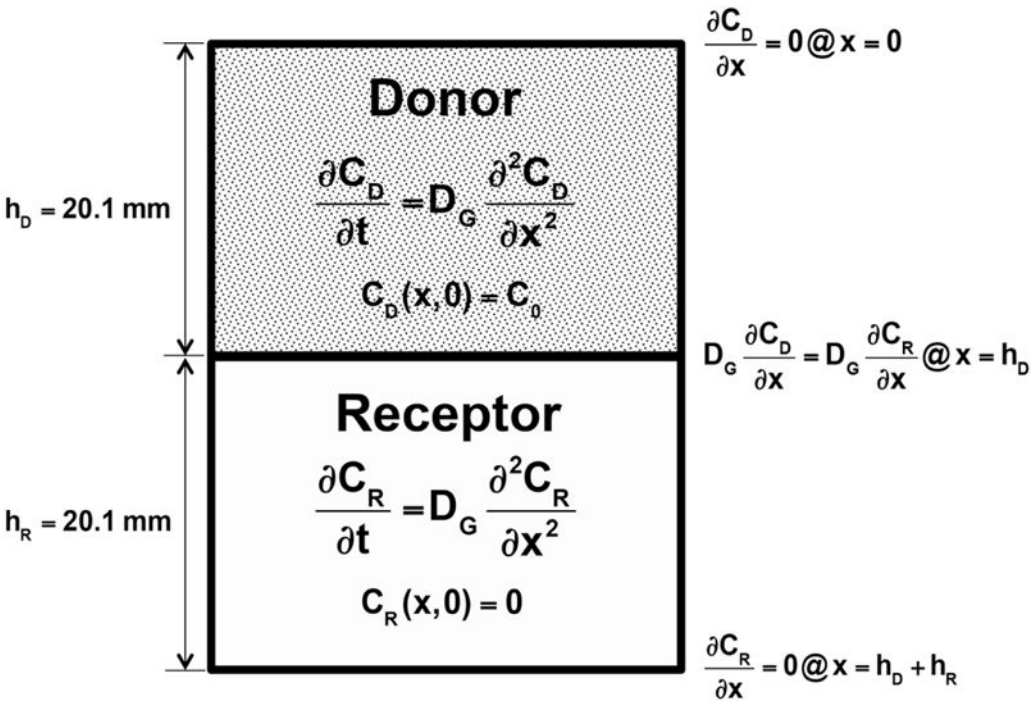

Figure 4.
Schematic of drug transport model for gel diffusion assay.

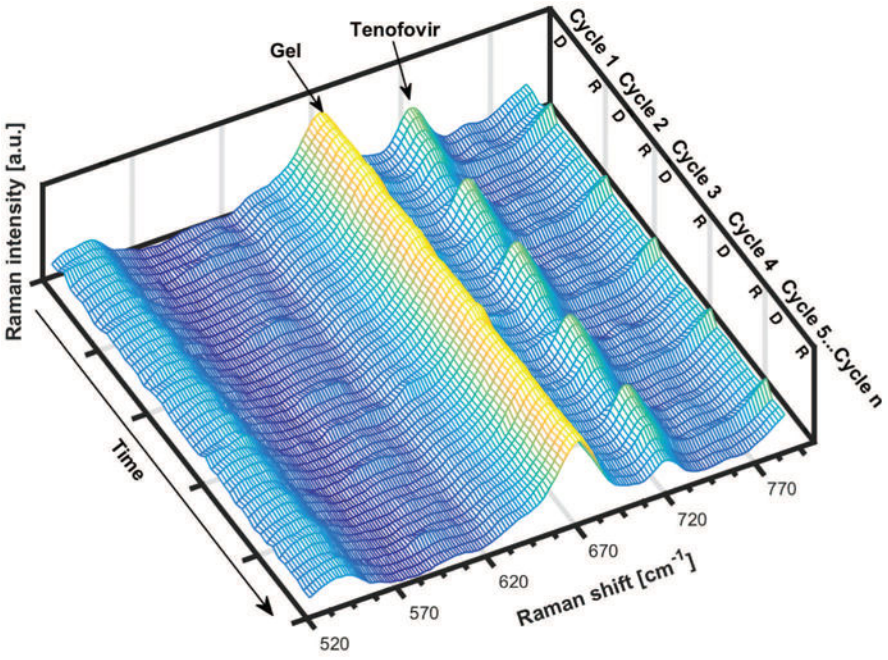

Figure 5.

Representative real-time Raman spectra acquired from the donor (D) and receptor (R) compartments over time. Spectra shown represent 5 cycles of measurements acquired successively; each cycle was acquired over the entire imaged length of the chamber starting at the end of the donor compartment and moving with 500 μm steps towards the opposite end of the receptor compartment. The total number of cycles obtained during each of the 24-h long experiments ranged from 50 to 70. The adenine peaks of tenofovir near 725 cm^{-1} decreased as the focal position moved from the donor to the receptor compartment, while the intensities of the gel (glycerol) peak near 676 cm^{-1} remained unchanged. Spectra were cropped for clarity of presentation.

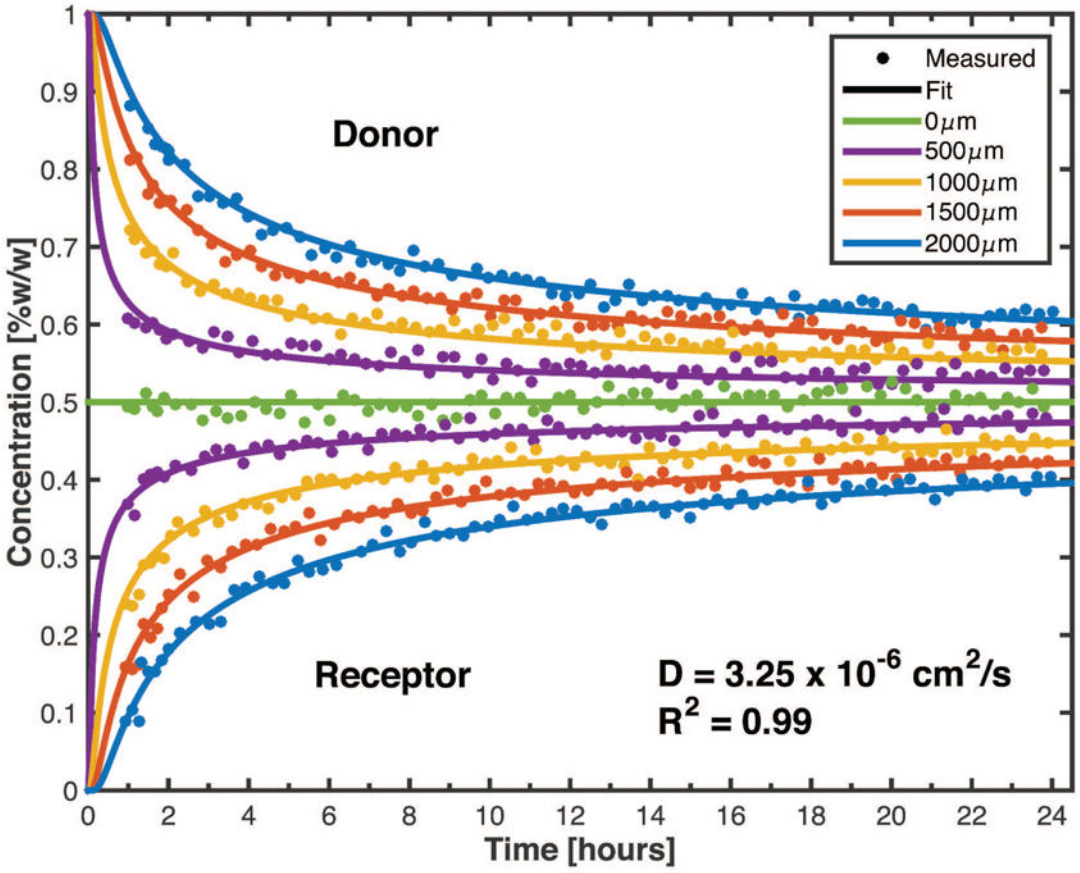

Figure 6.

Representative concentration profiles measured over time and space of an undiluted gel. The data were fitted with the compartmental PDE model (Figure 4) to obtain the diffusion coefficient.

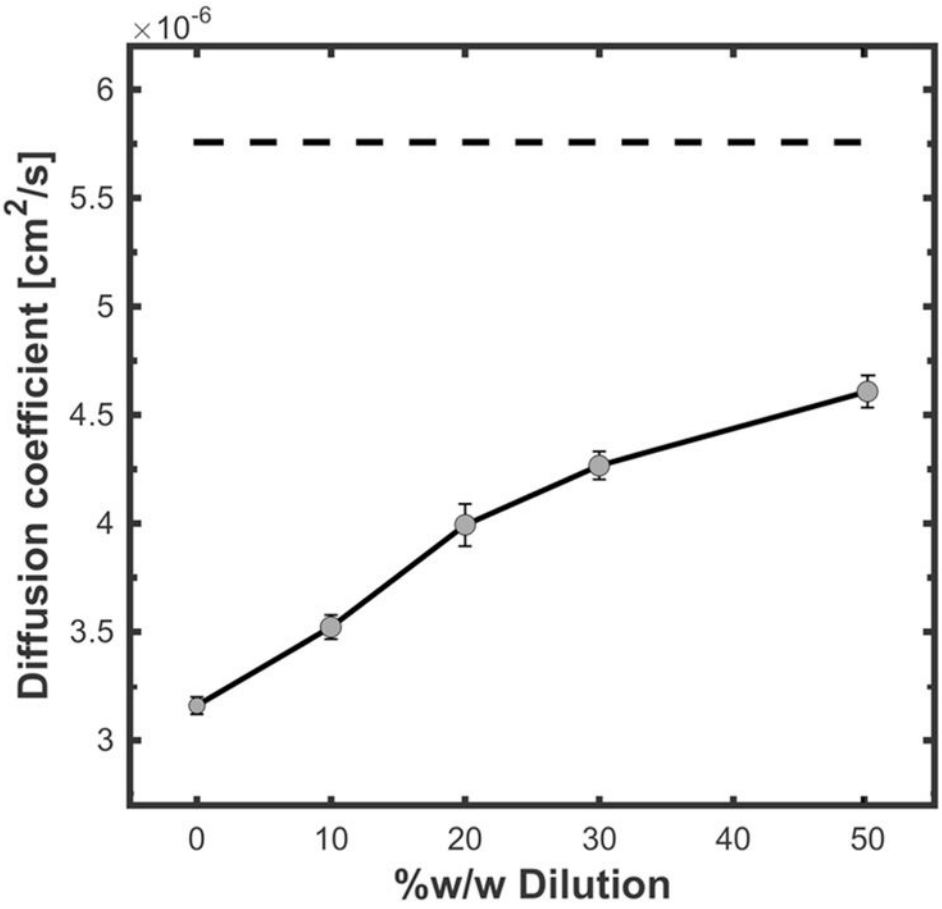

Figure 7.

Diffusion coefficients in gel versus dilution with vaginal fluid simulant. Each data point represents mean ± SE from 4–7 independent experiments. Dilution was defined as the weight by weight ratio of vaginal fluid simulant (VFS) to total weight of solution (VFS plus gel). Dashed line represents the diffusion coefficient of tenofovir in water (pH 4.2–4.4), as estimated by the Stokes-Einstein equation.

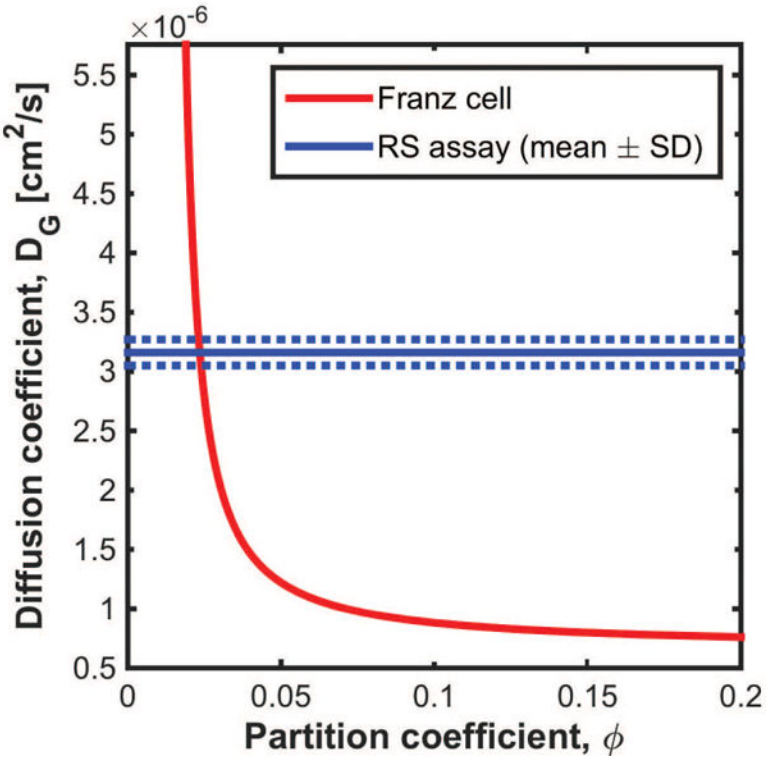

Figure 8.

Comparison of diffusion coefficients derived using concentration profile data obtained here from the Raman spectroscopy(RS)-based assay and published drug release data for the same gel (Dezzutti et al, 2012) from the traditional Franz diffusion cell.

Table 1

Diffusion coefficients (D_G) of tenofovir for different gel dilutions with vaginal fluid simulant

Dilution (%w/w)	Diffusion Coefficients ± SD ($10^{-6}cm^2/s$)
0	3.16 ± 0.11
10	3.52 ± 0.11
20	3.99 ± 0.19
30	4.27 ± 0.13
50	4.61 ± 0.15